



Centrum voor Wiskunde en Informatica

REPORTRAPPORT

Direct Multifractal Spectrum Calculation from the Wavelet Transform

Zbigniew R. Struzik

Information Systems (INS)

INS-R9914 October 31, 1999

Report INS-R9914
ISSN 1386-3681

CWI
P.O. Box 94079
1090 GB Amsterdam
The Netherlands

CWI is the National Research Institute for Mathematics and Computer Science. CWI is part of the Stichting Mathematisch Centrum (SMC), the Dutch foundation for promotion of mathematics and computer science and their applications.

SMC is sponsored by the Netherlands Organization for Scientific Research (NWO). CWI is a member of ERCIM, the European Research Consortium for Informatics and Mathematics.

Copyright © Stichting Mathematisch Centrum
P.O. Box 94079, 1090 GB Amsterdam (NL)
Kruislaan 413, 1098 SJ Amsterdam (NL)
Telephone +31 20 592 9333
Telefax +31 20 592 4199

Direct Multifractal Spectrum Calculation from the Wavelet Transform

Zbigniew R. Struzik

CWI

P.O. Box 94079, 1090 GB Amsterdam, The Netherlands

ABSTRACT

We present a direct method of calculation of the multifractal spectrum from the wavelet decomposition. Information pertinent to singular structures in time series is captured by the WTMM method and the local effective Hölder exponent is evaluated locally for each singular point of the time series. The direct multifractal spectrum is obtained from the scaling of the histograms of the local effective Hölder exponent. In addition, we illustrate the possibility of estimation of the spectrum from the entire continuous wavelet transform.

1991 Mathematics Subject Classification: 80-08, 82-08, 92-08

1991 ACM Computing Classification System: H.1.1.m, I.1.m, J.2, J.3

Keywords and Phrases: multifractal analysis, wavelet transform, Hölder exponent

Note: This work has been carried out under the Impact project.

1. INTRODUCTION

The application of the wavelet transform (modulus maxima) representation of a signal to multi-fractal analysis has almost reached the status of a standard. The formalism developed by Arneodo et al in the early nineties [1, 2] has been extensively used to test many natural phenomena and has contributed to substantial progress in each domain in which it has been applied [3, 4, 5]. Nevertheless the respective methodology is intrinsically statistical in nature and provides only global estimates of scaling (of the moments of relevant quantity). While this is often a required property, there are cases when local information about scaling provides more relevant information than the global spectrum. This is particularly true for time series where scaling properties are non-stationary, whether it be due to intrinsic changes in the signal scaling characteristics or even boundary effects.

To address this problem we have introduced [6] a method of estimation of the *local* scaling exponent through the paradigm of the multiplicative cascade. We reveal the hierarchy of the scaling branches of the cascade with the wavelet transform modulus maxima tree, which has proved to be an excellent tool for the purpose [2, 7]. Contrary to the intrinsically instable local slope of the maxima lines, this estimate is robust and provides a stable, effective Hölder exponent, local in scale and position. From this an attempt is made in this paper to derive the multifractal spectra directly from log-histogram scaling evaluation, linking the local analysis with the global multifractal spectra approach. Almost as stable as the global scaling estimates from the partition functions method, the direct histogram of the effective Hölder exponent provides considerably more information about the relative density of local scaling exponents, and may prove to be an interesting alternative in multifractal spectra estimation.

The structure of the paper is as follows. Since the Wavelet Transform is central to both the partition function based multifractal formalism of Arneodo, Muzy and Bacry [2] as well as to our direct approach, necessary introduction is given. In section 2, we focus on the relevant aspects of the wavelet transformation, in particular the ability to characterise scale-free behaviour through the Hölder exponent. Together with the hierarchical scale-wise decomposition provided by the wavelet transform, it will enable us to reveal the scaling properties of the tree of the multiplicative cascading process. In section 3, we introduce a technical model enabling us to estimate the scale-free characteristic (the effective Hölder exponent) for the branches of such a process. In section 4, we use the derived effective Hölder exponent for the local temporal description of the time series characteristics at a given

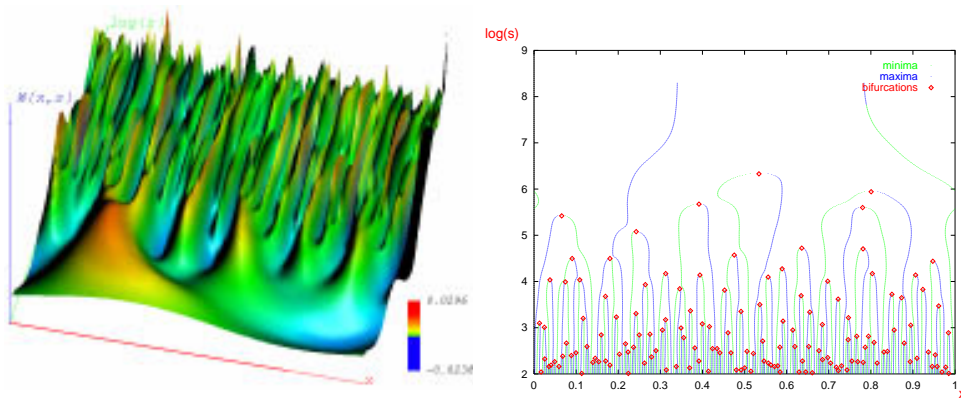


Figure 1: Left: Continuous Wavelet Transform representation of the random walk (Brownian process) time series. The wavelet used is the Mexican hat - the second derivative of the Gaussian kernel. The coordinate axes are: position x , scale in logarithm $\log(s)$, and the value of the transform $W(s, x)$. Right: The related WTMM representation.

resolution (scale). This is followed by an analysis of distributions of local h and the (scaling) evolution of the log-histogram and its relation to the standard partition functions based multifractal formalism. Section 5 closes the paper with conclusions.

2. CONTINUOUS WAVELET TRANSFORM AND ITS MAXIMA USED TO REVEAL THE STRUCTURE OF SINGULARITIES IN THE TIME SERIES

Conceptually, the wavelet transformation [8, 9] is a convolution product of the time series with the scaled and translated kernel - the wavelet $\psi(x)$, usually a n -th derivative of a smoothing kernel $\theta(x)$. Usually, in the absence of other criteria, the preferred choice is the kernel, which is well localised both in frequency and position. In this paper, we chose the Gaussian $\theta(x) = \exp(-x^2/2)$ as the smoothing kernel, which has optimal localisation in both domains.

The scaling and translation actions are performed by two parameters; the scale parameter s ‘adapts’ the width of the wavelet kernel to the *microscopic resolution* required, thus changing its frequency contents, and the location of the analysing wavelet is determined by the parameter b :

$$Wf(s, b) = \frac{1}{s} \int_{-\infty}^{\infty} dx f(x) \psi\left(\frac{x-b}{s}\right),$$

where $s, b \in \mathbf{R}$ and $s > 0$ for the continuous version (CWT).

The 3D plot in figure 1 shows how the wavelet transform reveals more and more detail while going towards smaller scales, i.e. towards smaller $\log(s)$ values. Therefore, the wavelet transform is sometimes referred to as the ‘mathematical microscope’, due to its ability to focus on weak transients and singularities in the time series. The wavelet used determines the optics of the microscope; its magnification varies with the scale factor s .

It can be shown [10] that for cusp singularities, the location of the singularity can be detected, and the related exponent can be recovered from the scaling of the Wavelet Transform, along the so-called *maxima line*, converging towards the singularity. This is a line where the wavelet transform reaches local maximum (with respect to the position coordinate). Connecting such local maxima within the continuous wavelet transform ‘landscape’ gives rise to the entire tree of maxima lines. Restricting oneself to the collection of such maxima lines provides a particularly useful representation [11] (WTMM) of the entire CWT. It incorporates the main characteristics of the WT: the ability to reveal the *hierarchy* of (singular) features, including the scaling behaviour. [2] Restricting oneself to the collection

of such maxima lines provides a particularly useful representation of the entire CWT. In particular, we have the following power law proportionality¹ for the wavelet transform of the cusp singularity in $f(x_0)$:

$$W^{(n)}f(s, x_0) \sim |s|^{h(x_0)} .$$

This is under the condition that the wavelet has at least n vanishing moments, i.e. it is orthogonal to polynomials up to degree n : $\int_{-\infty}^{+\infty} x^m \psi(x) dx = 0 \quad \forall m, 0 \leq m < n$.

Moreover, the wavelet transform and its WTMM representation can also be shown to be invariant with respect to the rescaling/renormalisation operation [7, 2, 15, 14]. This property makes it an ideal tool for revealing the renormalisation structure of the (hypothetical) multiplicative process underlying the analysed time series.

2.1 Multifractal Formalism on the WTMM Tree

The WTMM tree has been used for defining the partition function based multifractal formalism [2]. It uses the moments q of the measure distributed on the WTMM tree to obtain the dependence of the scaling function $\tau(q)$ on the moments q :

$$\mathcal{Z}(s, q) \sim s^{\tau(q)} .$$

The $\mathcal{Z}(s, q)$ is the partition function of the q -th moment of the measure distributed over the wavelet transform maxima at the scale s considered:

$$\mathcal{Z}(s, q) = \sum_{\Omega(s)} (Wf\omega_i(s))^q , \tag{2.1}$$

where $\Omega(s) = \{\omega_i(s)\}$ is the set of all maxima $\omega_i(s)$ at the scale s , satisfying the constraint on their local logarithmic derivative in scale [16]. (The local slope bound used throughout this paper is $|\check{h}| \leq 2$.)

Intuitively, since the moment q has the ability to select a desired range of values: small for $q < 0$, or large for $q > 0$, the scaling function $\tau(q)$ globally captures the distribution of the exponents $h(x)$ - weak exponents are addressed with large negative q , while strong exponents are suppressed and effectively filtered out. For the large positive q , the opposite takes place (and strong exponents are addressed while weak exponents are effectively filtered out).

This dependence may be linear indicating that there is only one class of singular structures and related exponent, or it can have a slope non-linearly changing with q . In the latter case, the local tangent slope to $\tau(q_*)$ will give the corresponding exponent, i.e. $h(q_*)$, with its related dimension marked on the ordinate axis $C = D(h(q_*))$, where $\tau(q_*) = h(q_*)q_* + C$. The set of values C , i.e. dimensions $D(h(q_*))$ for each value of h selected with q_* is the so-called spectrum of the singularities $D(h)$ of the fractal signal. Formally, the transformation from $\tau(q)$ to $D(h)$ is referred to as the Legendre transformation:

$$\frac{d\tau(q)}{dq} = h(q) ,$$

$$D((h(q)) = q h(q) - \tau(q) .$$

¹One should bear in mind that the above relation is an approximate case for which exact theorems exist [12]. In particular, we will restrict the scope of this paper to Hölder singularities for which the local and pointwise Hölder exponents are equal [13]. Thus we will not take into consideration the ‘oscillating singularities’ (e.g. $x^\alpha \sin(1/x^\beta)$) requiring two exponents [12, 14]. Nevertheless, it is sufficient for our purpose to state that the continuous wavelet transform can be used for characterising the Hölder singularities in the time series even if masked by the polynomial bias.

Note that even though the method uses the maxima tree containing full local information about the singularities, this is lost at the very moment the partition function is computed. Therefore, there is no explicit local information present in the scaling estimates; τ , h or D , and all these are global statistical estimates. This is also where the strength of the partition function method lies - global averages are much more stable than local information and in some cases all that it is possible to obtain.

Indeed, it is generally not possible to obtain local estimates of the scaling behaviour other than in the case of isolated singular structures from the WT. A typical example of the evolution of the maximum line along scale is shown in figure 2. It is not possible to evaluate the slope of the plot, not even on the selected range of scales. This is why we introduced [6] an approach circumventing this problem while retaining local information - a local effective Hölder exponent in which we model the singularities as created in some kind of a collective process of a very generic class.

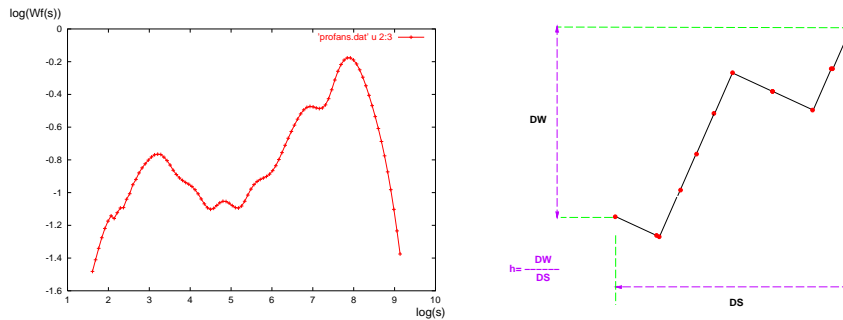


Figure 2: Left: It is impossible to evaluate the scaling exponent for an arbitrary maximum line participating in a complex process: a real file example of a maximum line. Right: The local effective Hölder exponent estimate takes the effective difference in the logarithm of the density of the process with respect to the logarithm of the scale difference along the process path.

3. ESTIMATION OF THE LOCAL, EFFECTIVE HÖLDER EXPONENT USING THE MULTIPLICATIVE CASCADE MODEL

We have shown in the previous section that the wavelet transform and in particular its maxima lines can be used in evaluating the Hölder exponent in isolated singularities. In most real life situations, however, the singularities in the time series are not isolated but densely packed. The logarithmic rate of increase or decay of the corresponding wavelet transform maximum line is usually not stable but fluctuates, following the action of the (hypothetical, multiplicative) process involved.

To capture the fluctuations and estimate the related exponents (to which we will refer to as an *effective* Hölder exponent of the singularity), we will model the singularities as created in some kind of a collective process of a very generic class - the multiplicative cascade model. Each point of this cascade is uniquely characterised by the sequence of weights $(s_1 \dots s_n)$ taking values from the (binary) set $\{1, 2\}$, and acting successively along a unique process branch leading to this point. Suppose that we denote the density of the cascade at the generation level F_i (i running from 0 to max) by $\kappa(F_i)$, we then have

$$\kappa(F_{max}) = p_{s_1} \dots p_{s_n} \kappa(F_0) = P_{F_0}^{F_{max}} \kappa(F_0)$$

and the local exponent is related to the rate of increase of the product $P_{F_0}^{F_{max}}$ over the gained scale difference. In any experimental situation, the weights p_i are not known and h has to be estimated. This can be simply done using the fact that for the multiplicative cascade process, the effective product of the weighting factors is reflected in the difference of logarithmic values of the densities at F_0 and F_{max} along the process branch:

$$h_{F_0}^{F_0} = \frac{\log(\kappa(F_{max})) - \log(\kappa(F_0))}{\log((1/2)^{max}) - \log((1/2)^0)}.$$

The densities along the process branch can be estimated with the wavelet transform, using its remarkable ability to reveal the entire process tree of a multiplicative process [7]. It can be shown that the densities $\kappa(F_i)$ corresponds with the value of the wavelet transform along the maxima lines belonging to the given process branch. The estimate of the effective Hölder exponent becomes:

$$\hat{h}_{s_{lo}}^{s_{hi}} = \frac{\log(Wf\omega_{pb}(s_{lo})) - \log(Wf\omega_{pb}(s_{hi}))}{\log(s_{lo}) - \log(s_{hi})},$$

where $Wf\omega_{pb}(s)$ is the value of the wavelet transform at the scale s , along the maximum line ω_{pb} corresponding to the given process branch. Scale s_{lo} corresponds with generation F_{max} , while s_{hi} corresponds with generation F_0 , (simply largest available scale in our case).

4. EMPLOYING THE EFFECTIVE HÖLDER EXPONENT IN GLOBAL SPECTRA ESTIMATION

Such an estimated local $\hat{h}(x_0, s)$ can be depicted in the temporal fashion, for example with a background colour, as we have done in figure 3. The first example time series is a computer generated sample of fractional Brownian motion with $H = 0.6$. It shows almost monochromatic behaviour, centred at $H = 0.6$. The colour green is dominant. There are, however, several instances of darker green and light blue indicating locally smooth components.

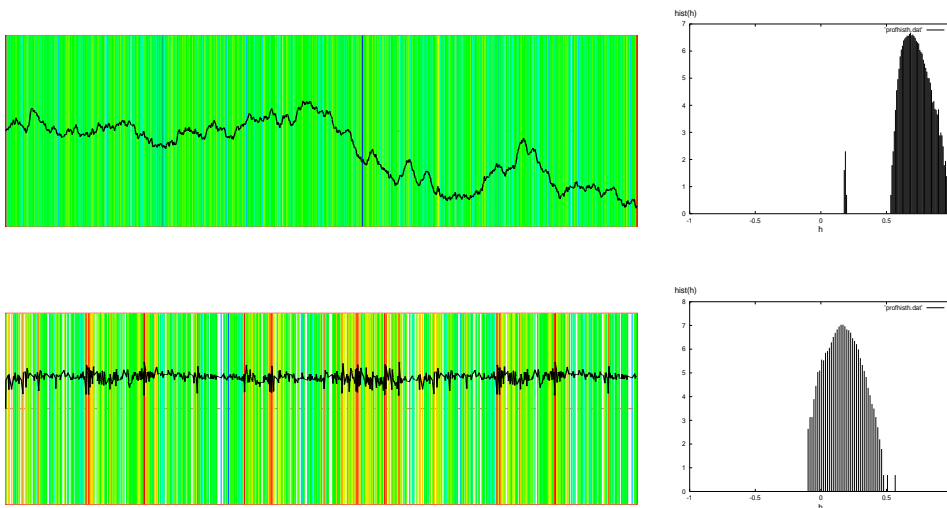


Figure 3: Left: Example time series with local Hurst exponent indicated in colour: fBm with $H = 0.6$ and the record of healthy heart interbeat intervals. The background colour indicates the Hölder exponent locally, centred at the Hurst exponent at green, colour goes towards blue for higher \hat{h} and towards red for lower \hat{h} . Right: The corresponding log-histograms of the local Hölder exponent.

The second example is a record [17] of heartbeat intervals recorded from a healthy human heart and it shows an intricate structure of interwoven singularities at various strengths. This behaviour has been recently reported [18] to correspond with the multifractal behaviour of the heartbeat. The green is centred at $\hat{h} = 0.1$. To the right of figure 3, the log-histograms are shown of the Hölder exponent displayed in the colour plots. They are made by taking the logarithm of the measure in each histogram bin. This conserves the monotonicity of the original histogram, but allows us to

compare the log-histograms with the spectrum of singularities $D(h)$. By following the evolution of the log-histograms along scale we will be able to extract the spectrum of the singularities $D(h)$.

4.1 Scale-wise Evolution of the Effective Hölder Exponent

In addition to one scale plot showing the colour spectrum of singular behaviour, we can also see the scale position locations where the effective Hölder exponent is near a particular value. We show an example *band* of $\hat{h}_\epsilon(s)$ of width $\epsilon = 0.02$, by selecting $\hat{h} = -0.5 \pm 0.01$ in figure 4 for the record of white noise. The number of locations that fall within the band range visibly grows with scale and this growth determines the dimension $D(h)$ which can be associated with the particular \hat{h} , at the band resolution ϵ .

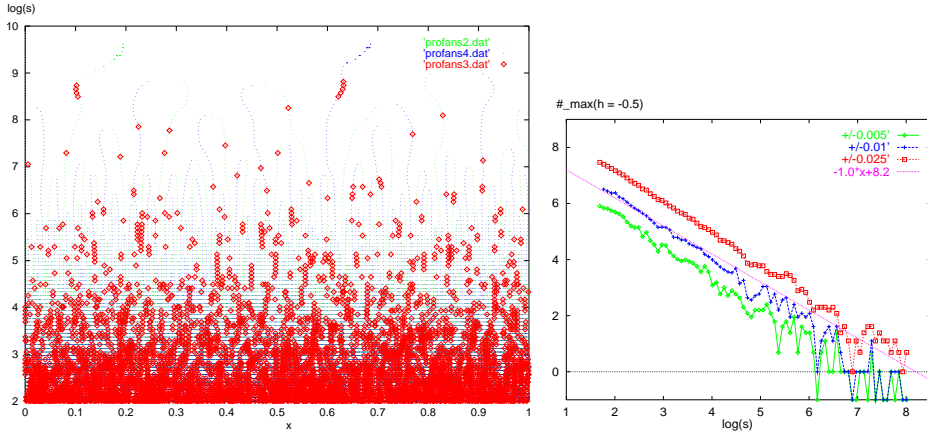


Figure 4: Left: WTMM representation of a sample of white noise. The maxima are highlighted where the effective Hölder exponent reaches a particular value of $\hat{h} = -0.5 \pm 0.01$, i.e. $\epsilon = 0.02$. Right: for three values of the band width $\epsilon = 0.01$, $\epsilon = 0.02$, $\epsilon = 0.05$, the logarithm of the sum of the highlighted maxima is shown for each scale with respect to the $\log(s)$ axis. Consistent scaling of -1 rate is shown for *supremum* of $\epsilon = 0.02$ plot.

Such $D(h)$ can be estimated for the entire range of h , resulting in the so-called *spectrum of singularities*. It is a standard way of visualising the distribution of singularities - it gives the (fractal) dimension $D(h)$ of the supporting set of singularities for each exponent value h in the time series.

$$D(\hat{h}) = \dim(\{x_0\} : Tf(x - x_0) \sim |x - x_0|^{h(x_0)}) \sim \lim_{\epsilon \rightarrow 0} \lim_{s_{lo} \rightarrow 0} \frac{\log(\mu_\epsilon(\hat{h}(s_{lo})))}{\log(s_{lo})},$$

where μ_ϵ is the measure of the total number of locations (selected maxima) that fall within the band of size ϵ at a particular scale location s_{lo} . One additional modification to the scheme is the linear correction on the ϵ band width. It is meant to compensate for the decreasing scale range when shorter scale spans are considered. The ϵ_{mod} used is thus $\epsilon_{mod} * \log(s_{lo}/s_{hi})$.

The dimension $D(\hat{h})$ is evaluated in the standard way from the scaling of the log-log plot, as in figure 4 right. Obviously the width of the band of the exponents is a parameter of choice, (is subject to arbitrary choice) but this does not affect the slope of the log-log line within the realistic range of the ϵ . Three example log-log plots for three values of $\epsilon = .005$, $\epsilon = .01$, $\epsilon = .025$, are shown in 4 right. The slope of the log-log plot remains practically independent of the band width, this is especially true towards the small scale limit. The vertical shift in log-log plots is of course due to the decrease/increase of the maxima points within the selected band with its width decreased/increased. Similarly the variance of the log-log plot visibly increases with the decreasing band width.

4.2 Direct spectra from the (bands of) the Effective Hölder Exponent on the WTMM tree

Calculation/evaluation of direct spectra from the ϵ bands of the Hölder exponent simply accounts for covering the entire range of the local effective Hölder exponents detected on the maxima tree. In figure 5, we show the entire $D(\hat{h})$ spectra evaluated for the white noise sample of 16k length and for the record of healthy human heartbeat intervals of equal length. We used the band width of $\epsilon = \pm 0.01$.

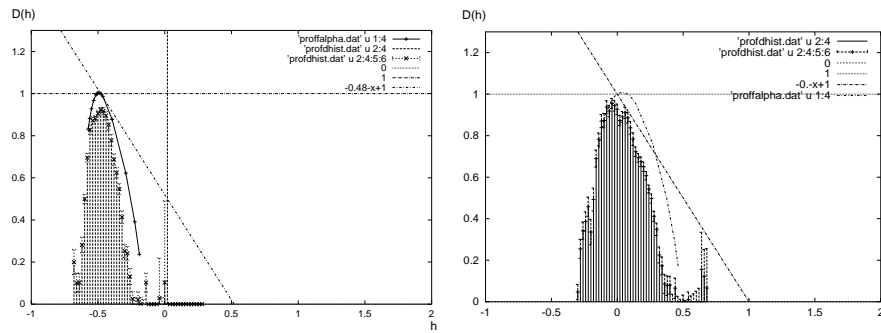


Figure 5: The multifractal spectrum calculated directly from the scaling of the histogram of the Hölder exponent on the maxima tree. Left for the white noise, right for the heartbeat intervals record. Band width 0.01.

The width of the spectrum of white noise is non-zero, as is inevitable for the finite length sample; still the heartbeat sample clearly shows considerably wider spectrum confirming the finding reported in [18].

Due to the fact that it relies on selecting a very narrow band of exponents, this procedure is, however, inherently sensitive to the choice of parameters such as the band width and the density of sampling of the scale axis. While the latter equally affects the partition function method, it does not pose any serious limitation since it can be increased at will, only adding to computation costs. In the case of the band width ϵ , only inherent to the direct method, we would, however, need to be ensured of some elementary degree of stability. The experiments indicate that the spectrum obtained remains stable for a wide choice of ϵ without loss of quality. An example is shown in figure 6 where spectra are calculated with $\epsilon = 0.02$, $\epsilon = 0.01$, $\epsilon = 0.005$.

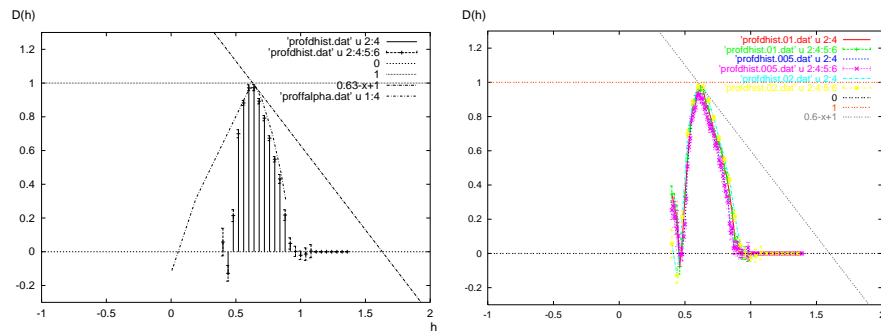


Figure 6: Left: The direct multifractal spectrum of the fBm sample of $H=0.6$ is not corrupted by the ‘outliers’ - the end of the sample singularities. as is the standard partition function method included for comparison. Right: The direct multifractal spectrum shows reasonable stability with respect to varied band width ϵ . Shown are overlapped cases $\epsilon = 0.02$, $\epsilon = 0.01$, $\epsilon = 0.005$.

At the cost of the slightly lower stability, we, however, obtain the advantages of the direct spectrum calculation. The spectrum better captures local variations in the scaling of the h bands, where the partition function method provides only rough, ‘outline’ information about the $D(h)$ spectrum. In

particular, the partition function spectrum can be dramatically corrupted by outliers (e.g. the end of the sample singularities, resulting from the linear trend present in the sample). The direct method seems to be much less prone to such behaviour. An experimental verification of this is shown in figure 6. Both types of spectra are calculated for the record of slightly correlated fBm of $H=0.6$. This sample contains some effective linear trend in it which results in the ‘trivial’ end of the sample singularities. The partition function method is inherently unable to distinguish these singularities resulting in a wide spectrum which can easily be suspected to be of multifractal origin. To the contrary the direct spectrum quickly falls off for the singularities lower than $H = 0.6$.

4.3 Direct spectra from the (bands of) the Effective Hölder Exponent on the entire CWT

We have already mentioned that the procedure of direct estimation of $D(h)$ is inherently unstable due to selecting a very narrow band of exponents, and thus a small subset of the maxima lines per scale level. This is the reason why it provides considerably less stable scaling estimates than the partition function method which is actually at the other extreme, taking *all* the maxima as the support for the measure of which the moments are calculated.

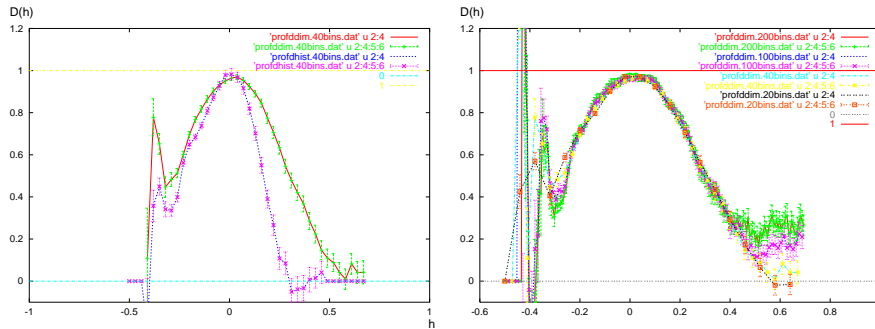


Figure 7: Left: The multifractal spectrum calculated directly from the scaling of the ϵ band of the Hölder exponent on the entire CWT as compared to the same on the WTMM tree only. While the left part of the spectrum shows similar behaviour, the right part related to smooth behaviour departs largely from the WTMM case, possibly capturing some missing information. Right: CWT direct spectra show very good stability with respect to varied band width ϵ . Shown are overlapped cases $\epsilon = 0.03$, $\epsilon = 0.015$, $\epsilon = 0.006$, $\epsilon = 0.003$. Note the smaller h range used.

It seems possible to take a middle path in order to calculate more stable scaling estimates of the $D(h)$ in the direct way from the scaling of ‘selected’ maxima parts. This can be done by weighted selection, replacing the histogram box centred at \hat{h} and of ϵ width, with a smooth, say Gaussian, kernel of ϵ standard deviation, centred at \hat{h} . We have attempted this in a slightly different way, making use of the redundant information contained in the original CWT (as opposed to the WTMM used thus far). The comparison of the direct spectra obtained with both WTMM and the CWT suggest that the CWT may contain some information lacking in the WTMM, this is especially evident in the smooth part of the spectrum. Indeed, the maxima lines primarily restrict the representation to strongest cusp singularities, potentially leaving out the intermediate, relatively smoother behaviour. The CWT direct spectra show excellent stability with respect to the ϵ band width variation. In figure 7, we went down to spectacular $\epsilon = 0.003$ resolution and observed the main body of the spectrum conserved with only the background noise slowly increasing.

5. CONCLUSIONS

We have presented a method of direct multifractal spectrum calculation from the scaling of the ϵ bands of the local effective Hölder exponent. The method makes use of the local effective Hölder exponent estimates motivated by the multiplicative cascade paradigm, and implemented on the hierarchy of

the wavelet transform modulus maxima tree(WTMM) or directly on the CWT. The spectra obtained largely inherit the robustness and stability of the local exponent estimate, and provide direct access to scaling information superior to that of the standard partition function method. In particular the direct CWT based estimates show exceptional stability with respect to the selected band width ϵ and may also provide additional information to that captured in the WTMM based spectra. Both the WTMM and CWT based direct method of histogramming the local effective Hölder exponent may prove to be an interesting alternative in multifractal spectra calculation.

References

1. A. Arneodo, E. Bacry and J.F. Muzy, *PRL*, **67**, No 25, 3515 (1991).
2. A. Arneodo, E. Bacry and J.F. Muzy, *Physica A*, **213**, 232 (1995).
J.F. Muzy, E. Bacry and A. Arneodo, *Int. J. of Bifurcation and Chaos* **4**, No 2, 245 (1994).
3. A. Arneodo, A. Argoul, J.F. Muzy, M. Tabard and E. Bacry, *Fractals* **1**, 629 (1995).
4. A. Arneodo, E. Bacry, P.V. Graves and J.F. Muzy, *PRL*, **74**, No 16, 3293 (1995).
5. P.Ch. Ivanov, M.G. Rosenblum, C.-K. Peng, J. Mietus, S. Havlin, H.E. Stanley and A.L. Goldberger, *Nature*, **383**, 323 (1996).
6. Z. R. Struzik, in *Fractals: Theory and Applications in Engineering*, Eds: M. Dekking, J. Lévy Véhel, E. Lutton, C. Tricot, Springer Verlag, (1999).
7. Z.R. Struzik *Fractals* **3** No.2, 329 (1995).
Z.R. Struzik, *Thesis*, University of Amsterdam. (1996). Z.R. Struzik,
8. I. Daubechies, *Ten Lectures on Wavelets*, (S.I.A.M., 1992).
9. M. Holschneider, *Wavelets - An Analysis Tool*, (Oxford Science Publications, 1995).
10. S.G. Mallat and W.L. Hwang, *IEEE Trans. on Information Theory* **38**, 617 (1992).
11. S.G. Mallat and S. Zhong *IEEE Trans. PAMI* **14**, 710 (1992).
12. S. Jaffard and Y. Meyer, *Memoirs of AMS*, 123 (1996).
13. B. Guiheneuf and J. Lévy Véhel, *Proc. of Int. Wavelets Conference*, Tangier (1998).
14. A. Arneodo, E. Bacry and J.F. Muzy, *PRL*, **74**, No 24, 4823 (1995).
15. A. Arneodo, E. Bacry and J.F. Muzy(1994): Solving the Inverse Fractal Problem from Wavelet Analysis. *Europhysics Letters*, **25**, No 7, 479–484.
16. Z.R. Struzik, *CWI Report*, **INS-R9803**. Also see ‘Fractals and Beyond - Complexities in the Sciences’, M.M. Novak, Ed., World Scientific, 351 (1998).
17. *Heart Failure Database* (Beth Israel Deaconess Medical Center, Boston, MA).
18. P.Ch. Ivanov, M.G. Rosenblum, L.A. Nunes Amaral, Z.R. Struzik, S. Havlin, A.L. Goldberger and H.E. Stanley, *Nature* **399**, (1999).